BULLETIN OF THE EARTHQUAKE
RESEARCH INSTITUTE
Vol. 48 (1970), pp. 521-531

29. *Theoretical Seismograms of Spheroidal Type on the Surface of a Gravitating Elastic Sphere. V. Case of Gutenberg-Bullen A' Earth Model* (Continued).

By Tatsuo USAMI and Yasuo SATÔ,
Earthquake Research Institute.

(Read April 21, 1970.—Received April 25, 1970.)

1. Introduction

Since 1962 the period of free oscillation, phase and group velocities, common spectrum and resulting theoretical seismograms have been investigated using various earth models. A homogeneous elastic sphere [Satô et al. (1962), Usami and Satô (1964)], a homogeneous mantle and a homogeneous liquid core [Satô et al. (1968)] and Gutenberg-Bullen A' earth model [Satô et al. (1967a)] were treated in this course of study, and the surface disturbances due to the stress applied in a localized part on the spherical surface were calculated. For the case of a homogeneous mantle with a liquid core, the effect of radial and tangential stresses was compared using theoretical seismograms based on the contribution of all the modes having period larger than 5.0 sec. [Usami and Satô (1970), Satô et al. (1968)] and in this way the contribution of short waves in those cases was studied.

In the second paper of this series [Satô et al. (1967a)], the case of Gutenberg-Bullen A' earth model was investigated employing modes with radial mode number $i=1\sim10$ and proper periods longer than 80 sec. In this work fundamental features of the effect of gravity was made clear and in the calculated seismogram a new phase of surface wave named R_h was found, which was understood to be associated with radial higher modes $i=2$ and 3. In spite of well developed long waves general features did not resemble the actual seismograms, owing to the lack of short waves. In the present work, therefore, the fundamental and radial higher modes ($i=1\sim10$) with periods as short as 10 seconds are introduced in the calculation, the effect of such short period modes being studied.

2. Earth Model and Fundamental Quantities.

The same earth model as used in the second paper of this series [Satô et al. (1967a). Cited as paper II hereafter] is also adopted in the present paper. The radial variation of P and S wave velocities and of density appear in both graphical and tabular forms in an earlier paper [Usami and Satô (1965)].

The non-dimensional frequencies of the modes which have radial mode numbers $i=1\sim10$ and period between 10 and 80 sec were newly calculated using the method explained in paper II. Such values are graphically expressed in another paper [Usami et al. (1970b)]. The effect of gravity on these modes was proved to be negligibly small.

In paper II and another work by Usami et al. (1970b), the phase and group velocities calculated by asymptotic formulae

$$\begin{aligned} C/V_{so} &= \eta/(n+1/2) \\ U/V_{so} &= d\eta/dn \end{aligned} \tag{2.1}$$

are given in graphical forms. For the fundamental mode, the group velocity decreases with the period decrease and shows a minimum value 3.58 km/sec at period near 220 seconds. It increases again, attaining to its maximum value 3.96 km/sec near 60 seconds and then decreases again making minimum 2.87 km/sec near a period 18 seconds.

Common spectrum, which is a function of spatial and time characteristics of applied force, is calculated for both radial and colatitudinal components and is exhibited in Figures 1a and 1b. Since common spectrum is independent of the variables t, θ and φ, it may be used to calculate the displacement at all times and locations. Negligibly small values have been omitted from the figures in the interest of clarity. In the rectangular enclosures, some parts of the figure are given in enlarged forms. Comparison of the common spectrum in the present study with that in paper II shows that:

1) The maximum value of fundamental mode for the radial component in the present study is much larger than that in paper II. The relation is reverse for the colatitudinal component.

2) The ratio of amplitude of radial higher modes to fundamental mode is smaller in the present study than in the case treated in paper II.

3) In general, the present study shows simpler features than paper II.

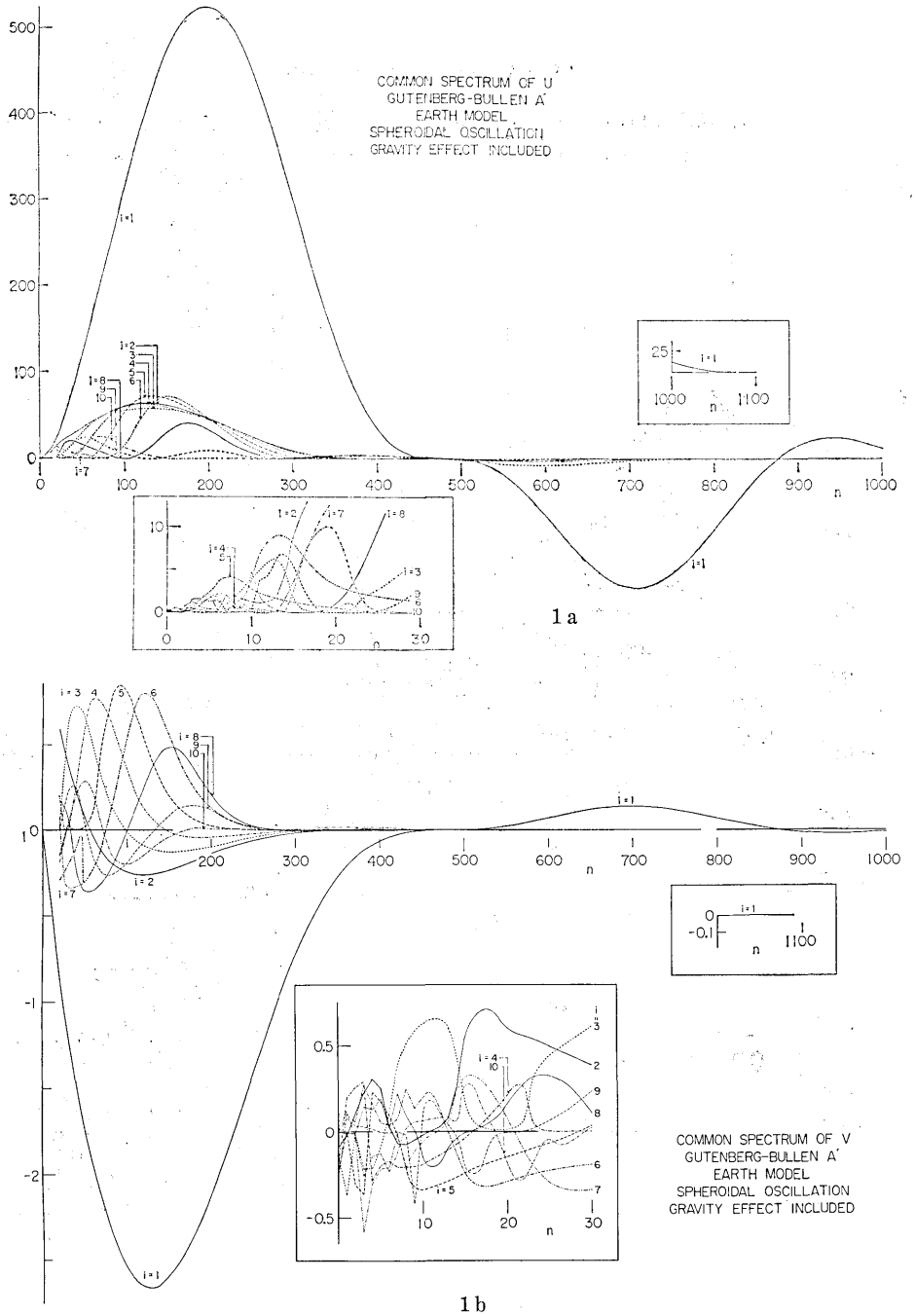

Fig. 1. Common spectrum of radial and colatitudinal components for radial modes $i=1\sim10$ as functions of the colatitudinal order number n. The ordinate scale is consistent with that in paper II. A part of the figure is shown in a rectangular enclosure in enlarged scale. The maximum colatitudinal order number n employed in the numerical work can be inferred from the Figure.

3. Theoretical Seismograms

A pure radial stress is assumed on the surface in a circular area around the pole. Its space distribution is, assuming the axial symmetry ($m=0$),

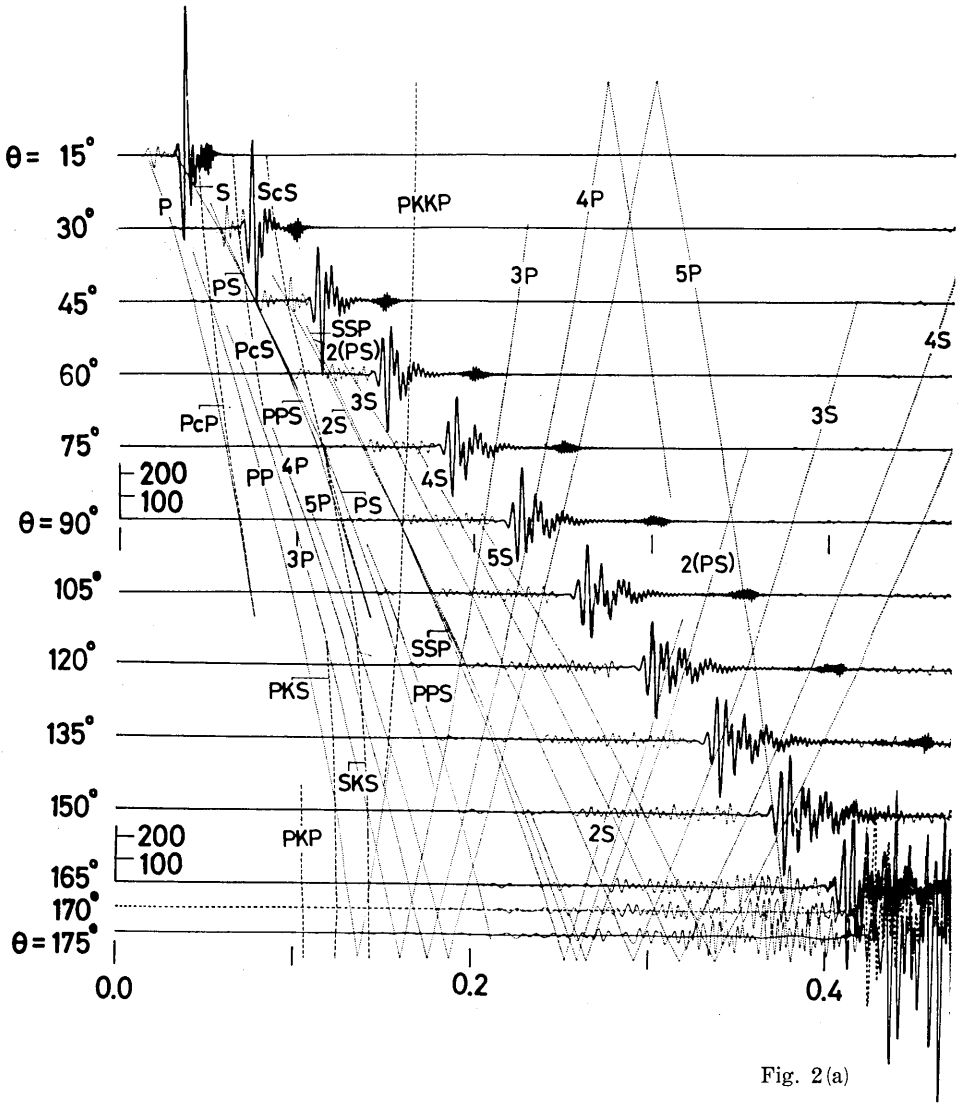

Fig. 2(a)

Fig. 2. Theoretical seismogram of spheroidal disturbances at 13 points on the surface of Gutenberg-Bullen A′ earth model. The solid line refers to $({}_1u_{1200})$ and $({}_1v_{1200})$, namely, to the sum of contributions from fundamental mode. The dotted curve expresses $({}_{10}u_{1200})$ and $({}_{10}v_{1200})$, that is, the sum of all the contributions from radial modes $i=1\sim10$.

$$\Phi^0(\cos\theta)=\begin{cases}1 & \theta<\theta_0 \\ 0 & \theta_0>\theta\end{cases} \quad (\theta_0=0.008 \text{ radian}) \tag{3.1}$$

The time function is

$$f(t)=\begin{cases}-1 & -t_1<t<0 \\ 1 & 0<t<t_1 \\ 0 & t_1<|t|\end{cases} \quad (t_1=0.002) \tag{3.2}$$

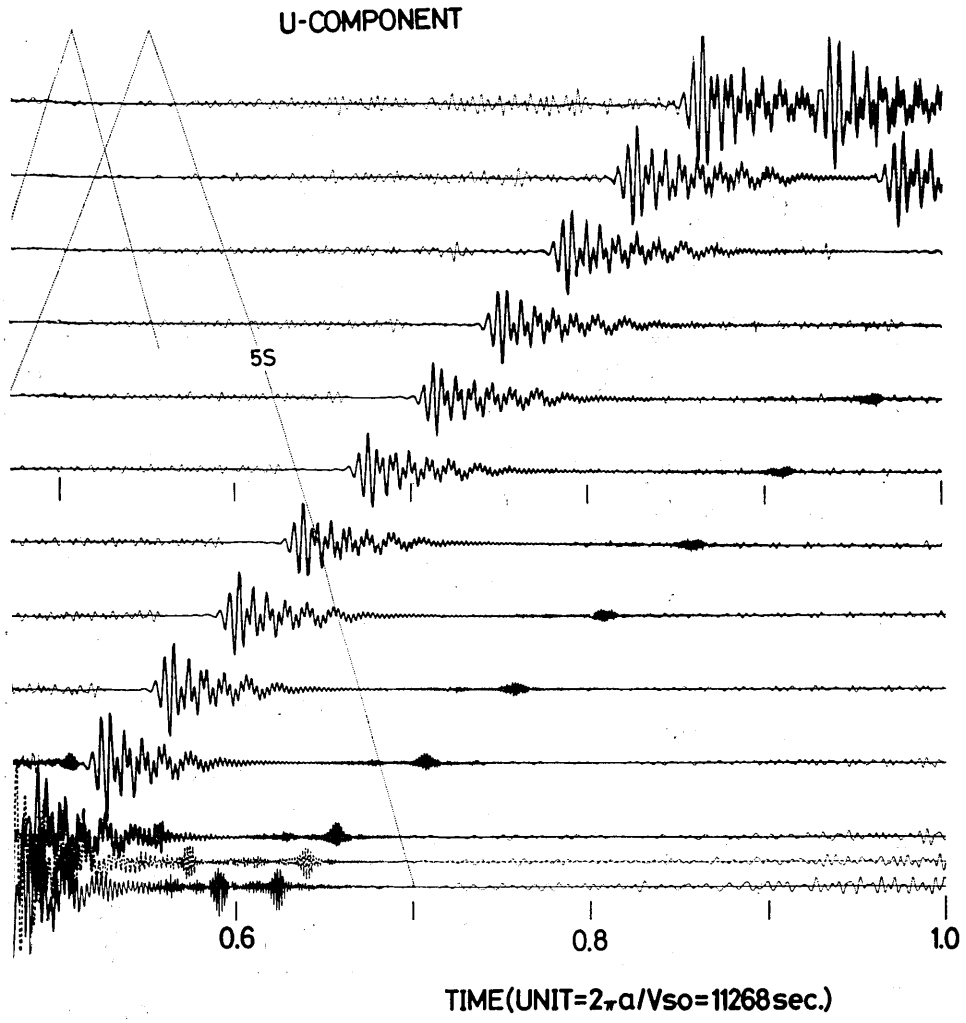

For example, $({}_iu_n)=\sum_{i=1}^{i}\sum_{n=0}^{n}{}_iu_n$. Predominant waves are Rayleigh waves. Expected arrival times of various body phases are shown in a form of travel time curve. As to the notation of wave, 2(*PS*), for example, means surface reflected wave *PPSS*. The unit of time is $2\pi a/Vso=11268$ sec.

and its Fourier transform is

$$f^*(t) = -4j \cdot \sin^2(pt_1/2)/p \tag{3.3}$$

The largest values of colatitudinal order number n employed in the synthesis can be inferred from the curves in Figure 1.

Theoretical seismograms were calculated at 13 points on the surface, that is, $\theta=15°$, $30°$, $45°$, $60°$, $75°$, $90°$, $105°$, $120°$, $135°$, $150°$, $165°$, $170°$ and $175°$ for the time interval $t=0.0005$ (0.0005) 1.0000. They

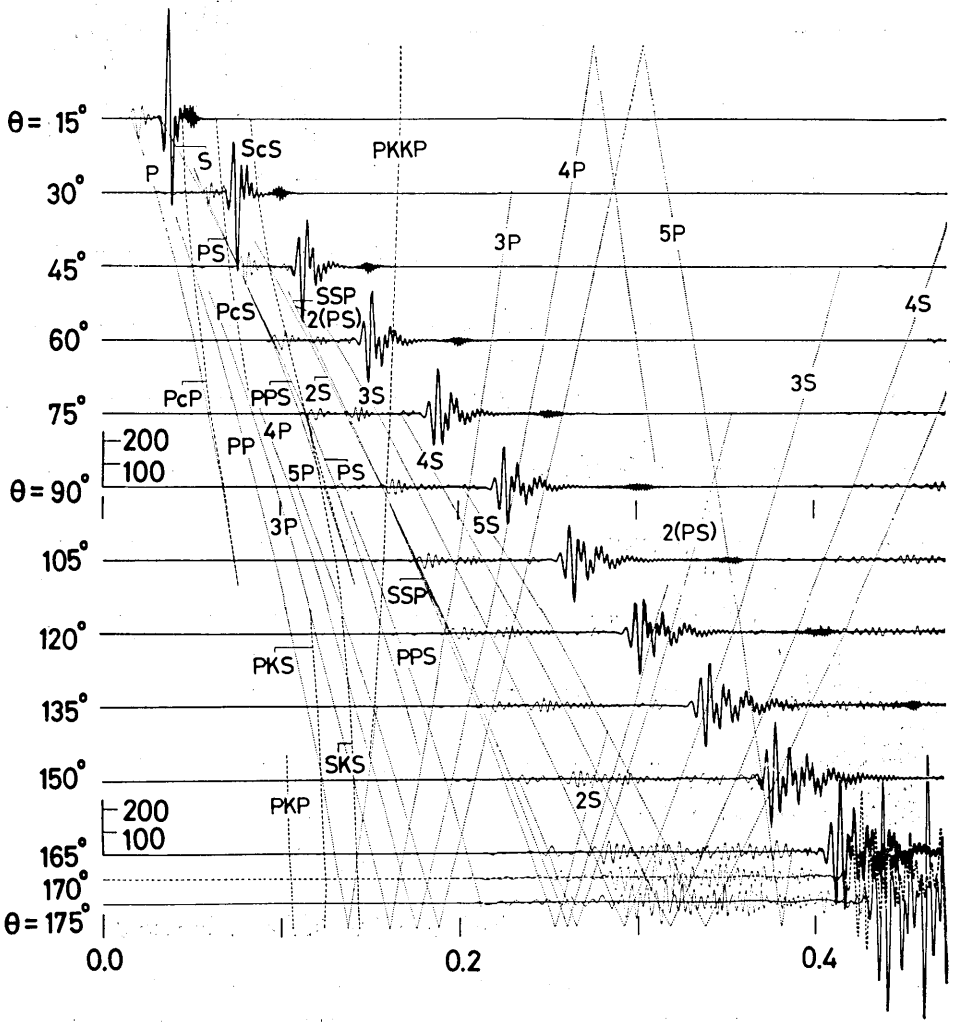

Fig. 2(b)

are shown in Figures 2a and 2b. $2\pi a/V_{so}=11268$ sec, the time for the S wave to circle the globe, is taken as the unit of time. V_{so} is the S wave velocity on the surface.

In Figure 2, thin dotted curves refer to $({}_{10}u_{1200})$ and $({}_{10}v_{1200})$ and solid curves to $({}_{1}u_{1200})$ and $({}_{1}v_{1200})$. For the epicentral distance $\Delta=170°$, broken line is used instead of solid line in the interest of clarity. The ordinate scale is consistent to that in paper II. Arrival times of various body waves is given in a form of travel time curves. Figure 2 indicates that:

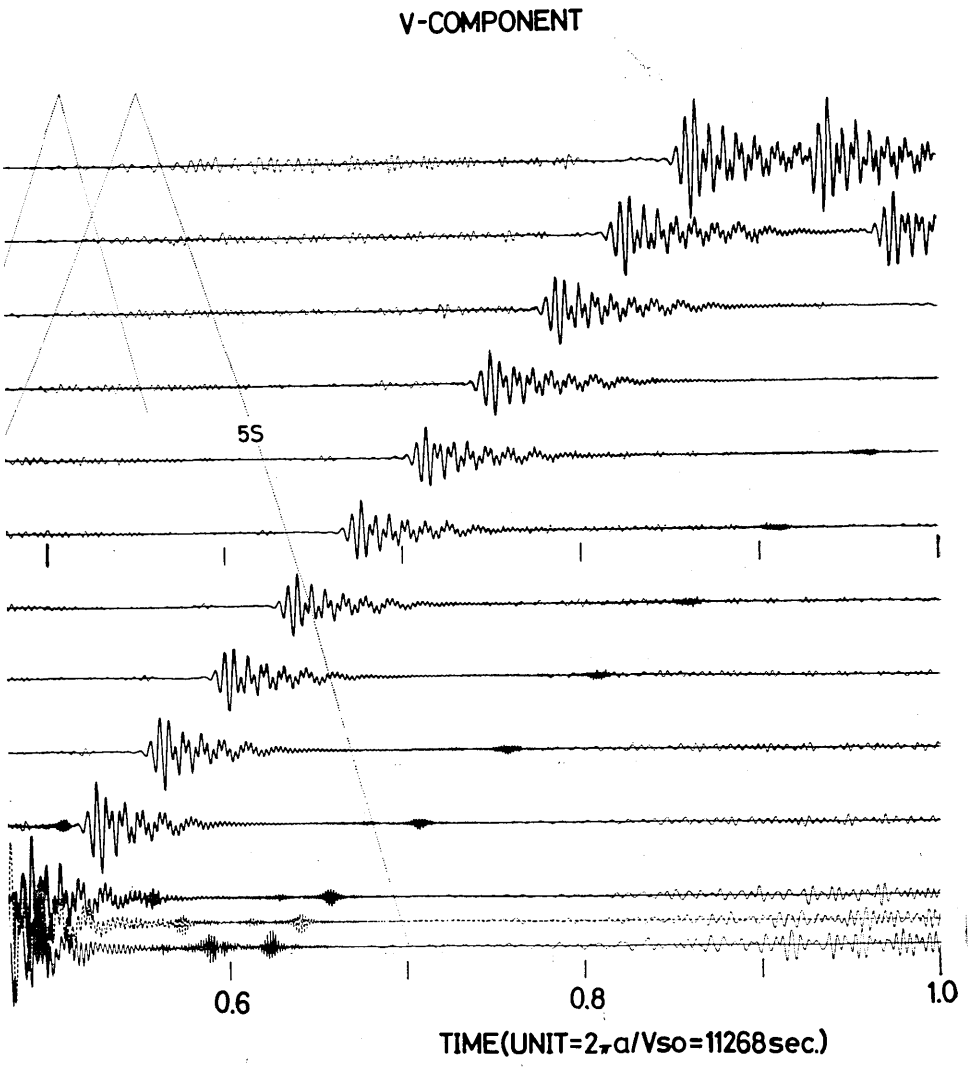

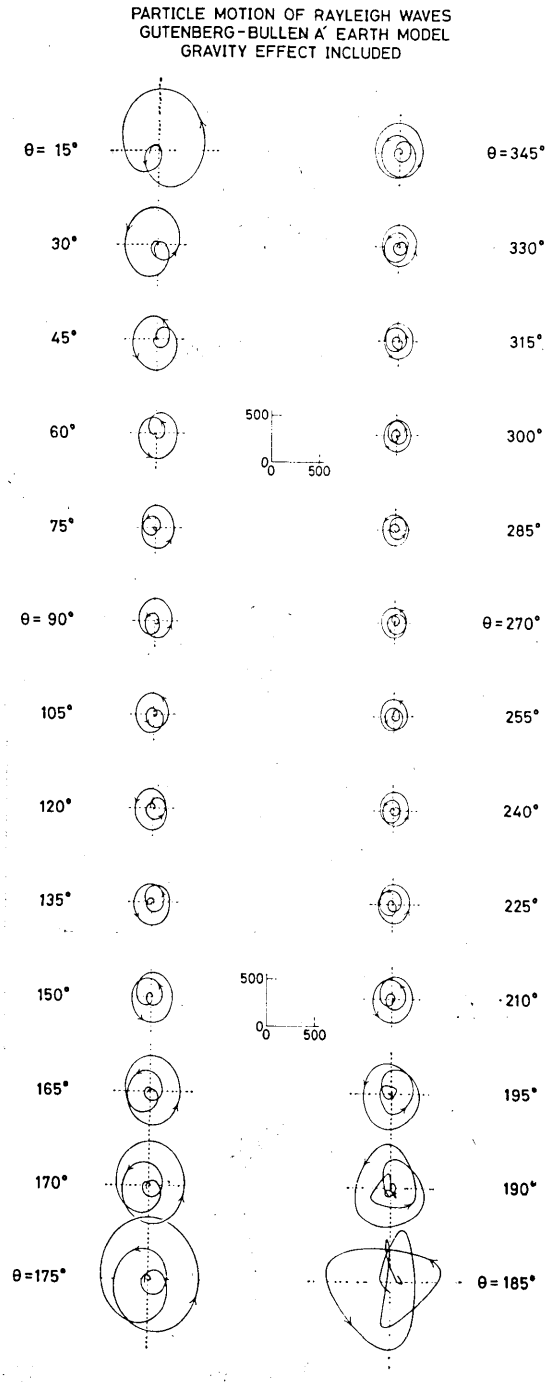

Fig. 3. Particle motion of the initial part of Rayleigh waves. The pattern of locus shows typical features of Rayleigh wave. The scale is consistent to that of Fig. 2.

1) Short period waves are more predominant in the present case than in paper II, reflecting the time and space function of the applied force.

2) Amplitude of Rayleigh waves in the present case is larger than in the case of paper II. Near the end of surface wave, shorter period waves of smaller amplitude with a shuttle shape appears very clearly. This wave corresponds to the fundamental mode with about 18 second period, and its arrival time can be interpreted by the minimum group velocity.

3) Direct waves, reflected, refracted and diffracted waves at the core boundary, and reflected waves from the free surface are identified on the theoretical seismograms and their arrival times show good agreement with travel time curve obtained from a simple theory of geometrical optics. Among body waves, the onsets of multiple reflected S waves at the surface such as $2S$, $3S$, $4S$ and $5S$ are identified in the theoretical seismograms.

4) The difference between solid and dotted curves means the contributions from radial higher modes and is small during the passage of Rayleigh waves. This illustration confirms that the fundamental mode is closely related to the surface waves and radial higher modes to body waves.

5) Surface waves named R_h in paper II are not found in the present case. This wave stems from maximum and minimum group velocities of radial higher modes $i=2$ and 3 and has a period of several hundred seconds. In the present case, the common spectrum is small for this period range, which fact explains the absence of this kind of wave.

The loci of particle motion due to Rayleigh waves at various points on the surface are illustrated in Figure 3. These show characteristics typical to Rayleigh waves such as 1) retrograde particle motion, 2) ratio of amplitude of vertical component to horizontal one being nearly equal to 1.4, the value for plane Rayleigh wave, and 3) rapid amplitude increase near the pole and antipole. Moreover, it is found in Figure 3 that the locus pattern becomes complicated and the number of loops increases with the epicentral distance. The initial part of Rayleigh waves at $\Delta=185°$ and 190° is disturbed by the coda of the waves propagated along the minor arcs of reverse side ($\Delta=175°$ and 170° respectively) and shows an irregular locus pattern.

The numerical work was carried out mainly by HITAC 5020E at the Computer Centre of the University of Tokyo and partly by IBM 7090 through the courtesy of UNICON, to which our sincere thanks are due.

References

SATÔ, Y., T. USAMI and M. EWING, 1962, Basic Study on the Oscillation of a Homogeneous Elastic Sphere. IV. Propagation of Disturbances on the Sphere, *Geophys. Mag.*, **31**, 237-242.

SATÔ, Y., T. USAMI and M. LANDISMAN, 1967a, Theoretical Seismograms of Spheroidal Type on the Surface of a Gravitating Elastic Sphere. II. Case of Gutenberg-Bullen A′ Earth Model, *Bull. Earthq. Res. Inst.*, **45**, 601-624.

SATÔ, Y., T. USAMI, M. LANDISMAN and T. ODAKA, 1968, Theoretical Seismograms of Spheroidal Type on the Surface of a Gravitating Elastic Sphere. III. Case of a Homogeneous Mantle with a Liquid Core, *Bull. Earthq. Res. Inst.*, **46**, 791-819.

USAMI, T. and Y. SATÔ, 1964, Propagation of Spheroidal Disturbances on a Homogeneous Elastic Sphere, *Bull. Earthq. Res. Inst.*, **42**, 273-287.

USAMI, T. and Y. SATÔ, 1970a, Theoretical Seismograms of Spheroidal Type on the Surface of a Gravitating Elastic Sphere. IV. Homogeneous Mantle with a Liquid Core Excited by Colatitudinal Force, *Bull. Earthq. Res. Inst.*, **48**, 351～362.

USAMI, T., Y. SATÔ and T. ODAKA, 1970b, Theoretical Seismograms and Earthquake Mechanism. Part I. Basic Principles. Part II Effect of Time Function on Surface Waves, *Bull. Earthq. Res. Inst.*, **48**, 533-579.

---

29. 重力均衡下にある弾性球の表面を伝わるスフェロイド型振動 V. グーテンベルグ・ブレン A′ モデルの場合 (続き)

地震研究所 宇佐美 龍 夫
佐 藤 泰 夫

1. 本シリーズの第 II 報において，グーテンベルグ・ブレン A′ モデルの場合について計算を行なったが，周期約 80 秒以上のモードのみを取扱ったので短周期の波については議論できなかった．今回は周期 11 秒以上のモードを加え合せて計算を行なった．
2. 地球モデルとしては第 II 報と同じものを使った．
3. 周期約 80 秒～11 秒のモードについて，スフェロイド型振動の周波数を $i=1$～10 について計算した．この範囲のモードに対する重力の影響は無視できる．
4. これから位相速度と群速度を計算した．群速度では周期 60～70 秒に極大が，約 17～18 秒に極小がみられる．
5. 実際の計算に当り，軸対称 ($m=0$) を仮定した．外力としては極のまわりに次のような表面に沿って働く半径方向の力を仮定した．

$$\Phi^0(\cos\theta)=\begin{cases}1 & \theta<\theta_0\\ 0 & \theta_0<\theta\end{cases}\qquad(\theta_0=0.008\ \text{ラヂアン})$$

$$f(t)=\begin{cases}-1 & -t_1<t<0\\ 1 & 0<t<t_1\\ 0 & t_1<|t|\end{cases}\qquad(t_1=0.002)$$

地球上の 13 点で時刻 $t=0.0005$ (0.0005) 1.0000 について理論地震記象を計算した．時間の単位は表面の S 波が地球を一周する時間で，11268 秒である．
6. コモン・スペクトルを求めて図示した．基準振動に対する高調波の振巾は第 II 報の場合より小さくなる．
7. 計算の結果，次のことが明らかになった．

a) 各種の実体波の発現時刻は理論的な走時とよく一致する.
b) 第 II 報に比し，実体波の始まりが明瞭となり，とくに $2S$, $3S$, $4S$, $5S$ といった波が見事に出現する.
c) 第 II 報で報告した R_h 波と記した波は現われない. これは此の周期と，外力の作用時間間隔が著しく離れているためである.
d) 表面波の終りに結び目のように短周期波がみえる. これは群速度極小 (周期 17～18 秒) に相当する波である.
e) 表面波のはじめの部分の粒子の運動を第 3 図に示した. これは平面境界のレイリー波の性質をよく示している.